Effect of dimensionality on the continuum percolation of overlapping hyperspheres and hypercubes

S. Torquato[a)]
Department of Chemistry, Department of Physics, Princeton Center for Theoretical Science, Princeton Institute for the Science and Technology of Materials, and Program in Applied and Computational Mathematics, Princeton University, Princeton, New Jersey 08544, USA

(Received 22 November 2011; accepted 9 January 2012; published online 3 February 2012)

We show analytically that the [0, 1], [1, 1], and [2, 1] Padé approximants of the mean cluster number S for both overlapping hyperspheres and overlapping oriented hypercubes are upper bounds on this quantity in any Euclidean dimension d. These results lead to lower bounds on the percolation threshold density η_c, which become progressively tighter as d increases and exact asymptotically as $d \to \infty$, i.e., $\eta_c \to 2^{-d}$. Our analysis is aided by a certain remarkable *duality* between the equilibrium hard-hypersphere (hypercube) fluid system and the continuum percolation model of overlapping hyperspheres (hypercubes). Analogies between these two seemingly different problems are described. We also obtain Percus-Yevick-like approximations for the mean cluster number S in any dimension d that also become asymptotically exact as $d \to \infty$. We infer that as the space dimension increases, finite-sized clusters become more ramified or "branch-like." These analytical estimates are used to assess simulation results for η_c up to 20 dimensions in the case of hyperspheres and up to 15 dimensions in the case of hypercubes. Our analysis sheds light on the radius of convergence of the density expansion for S and naturally leads to an analytical approximation for η_c that applies across all dimensions for both hyperspheres and oriented hypercubes. Finally, we describe the extension of our results to the case of overlapping particles of general anisotropic shape in d dimensions with a specified orientational probability distribution. © *2012 American Institute of Physics*. [doi:10.1063/1.3679861]

I. INTRODUCTION

The study of clustering behavior of particles in condensed-phase systems is of importance in phenomena such as nucleation, condensation of gases, gelation and polymerization, chemical association, structure of liquids, metal-insulator transition in liquid metals, conduction in dispersions, aggregation of colloids, and flow in porous media.[1–4] Percolation theory provides a powerful means of understanding such clustering phenomena. A prototypical model of continuum (off-lattice) percolation is a Poisson distribution (i.e., spatially uncorrelated) of equal-sized spheres. The percolation properties of this continuum model in one, two, and three dimensions in Euclidean space have been extensively studied.[4–19] Its transport and elastic properties, when used as models of two-phase heterogeneous media, have also been analytically characterized.[20–27] Two spheres are "connected" to one another if they overlap. Since the spheres are allowed to overlap, clusters of various sizes, shapes, and volumes are formed, as depicted in Figure 1. This model has been given a variety of names, including "fully penetrable spheres," "randomly overlapping spheres," the "Swiss-cheese model," and the "Poisson blob model." We will henceforth refer to this model as *overlapping hyperspheres* in d-dimensional Euclidean space $\mathbb{R}^d$. Observe that an affine (linear) deformation of an overlapping-hypersphere system in d orthogonal directions leads to an overlapping-hyperellipsoid system that possesses the same percolation threshold as the former, since the density remains invariant under an affine transformation.

For equal-sized overlapping hyperspheres of diameter D in $\mathbb{R}^d$ at number density ρ, defined to be the number of spheres per unit volume, it is convenient to introduce the reduced density η, which is defined by

$$\eta = \rho v_1(D/2), \tag{1}$$

where $v_1(R)$ is the d-dimensional volume of a sphere of radius R given by

$$v_1(R) = \frac{\pi^{d/2} R^d}{\Gamma(1 + d/2)}. \tag{2}$$

We will also consider percolation of overlapping oriented hypercubes of edge length D (see Fig. 2). The expression (1) for the reduced density η still applies when $v_1(D/2)$ is interpreted to be the volume of a cube with half-edge length $D/2$, i.e.,[28]

$$v_1(D/2) = D^d. \tag{3}$$

As in the case of overlapping hyperspheres, an affine deformation of a system of overlapping oriented hypercubes in d orthogonal directions leads to a system of overlapping oriented hyperparallelpipeds that possesses the same percolation threshold as the former.

The low-density expansion of the mean cluster number S (defined in Sec. II) encodes information about the pole of this function over its density domain, which determines the percolation threshold η_c. It has been observed that the [0, 1],

a)Electronic mail: torquato@electron.princeton.edu.

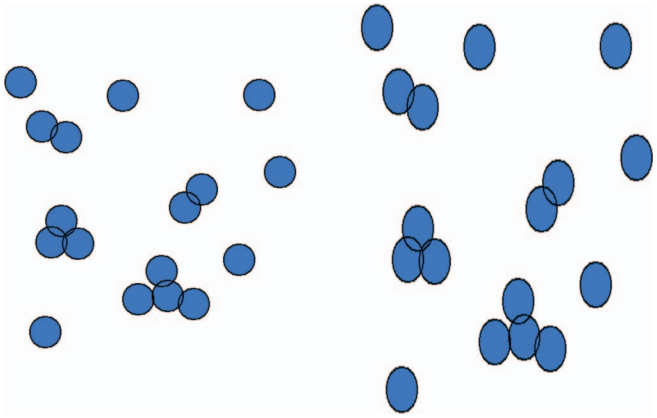

FIG. 1. Left Panel: Schematic of a system of overlapping circles (i.e., two-dimensional overlapping hyperspheres). Right Panel: Corresponding schematic of overlapping oriented ellipses obtained by an affine stretch of the overlapping-circle system in the vertical direction. The densities of the overlapping circle and ellipse systems are identical, since the density remains invariant under an affine transformation. Thus, the percolation thresholds of both systems are identical.

[1, 1], and [2, 1] Padé approximants of the mean cluster number S provide lower bounds on η_c for overlapping spheres in two and three dimensions (as determined by simulations) and become sharper as the order of the approximant increases.[19] In this paper, we show analytically that these Padé approximants are indeed lower bounds on S for both hyperspheres and hypercubes in any dimension d and that they become exact asymptotically as $d \to \infty$, i.e., $\eta_c \to 2^{-d}$. We also obtain Percus-Yevick-like approximations for the cluster number S that also become asymptotically exact as $d \to \infty$. Our bounds and approximations are compared to recent simulation results for η_c that span dimensions up to $d = 20$ in the case of overlapping hyperspheres[29,30] and up to $d = 15$ in the case of hypercubes.[30] Our analysis is aided by a striking *duality* between the equilibrium hard-hypersphere (hypercube) fluid system and the continuum percolation models of overlapping hyperspheres (hypercubes). Analogies between these seemingly disparate problems are discussed. Our investigation sheds light on the radius of convergence of the density expansion for S and naturally leads to an analytical approximation for η_c that applies across all dimensions. In Sec. IX, we describe the extension of our results to the case of overlapping particles of general anisotropic shape in d dimensions with a specified orientational probability distribution.

II. DEFINITIONS AND PRELIMINARIES

A. Connectedness criterion

Two spheres of radius $D/2$ are considered to be connected if they overlap, i.e., if the center of one lies within a spherical "exclusion" region of radius D centered around the other sphere (see Fig. 3). This connectedness criterion is captured by the "Mayer-f" connectedness function, which is a radial function given by

$$f(r) = \Theta(D - r), \tag{4}$$

where

$$\Theta(x) = \begin{cases} 1, & x \geq 0 \\ 0, & x < 0 \end{cases} \tag{5}$$

is the Heaviside step function. Thus, $f(r)$ is an indicator function for the exclusion region. The volume of the exclusion region $v_1(D)$ is given by the volume integral of $f(r)$, i.e.,

$$v_1(D) = \int_{\mathbb{R}^d} f(r) d\mathbf{r} = 2^d v_1(D/2). \tag{6}$$

By virtue of the fact that the spheres are Poisson distributed in space, it follows that the mean number of overlaps per sphere $\mathcal{N}$ is given by

$$\mathcal{N} = \rho v_1(D) = 2^d \eta. \tag{7}$$

Similarly, two oriented cubes of edge length D are taken to be connected if they overlap, i.e., if each Cartesian component of the displacement vector $\mathbf{r}$ between the centroids of the cubes is less than D, i.e., the connectedness exclusion-region

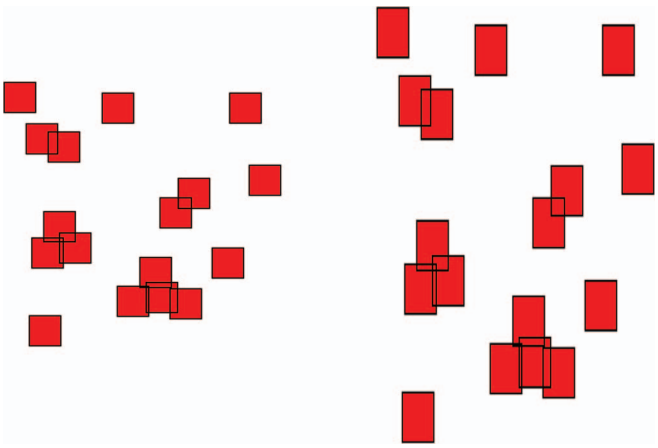

FIG. 2. Left Panel: Schematic of a system of overlapping oriented squares (i.e., two-dimensional overlapping hypercubes). Right Panel: Corresponding schematic of overlapping oriented ellipses obtained by an affine stretch of the overlapping-square system in the vertical direction. The densities for both systems are identical and hence their percolation thresholds are the same.

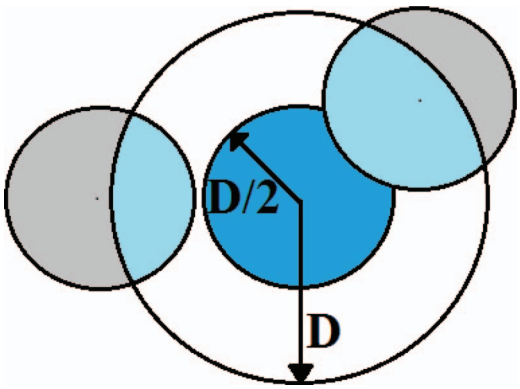

FIG. 3. Any center of a sphere of radius $D/2$ that lies within a spherical "exclusion" region of radius D centered around a central sphere of radius $D/2$ (dark blue) is connected to the central sphere. Whereas the leftmost sphere is not connected to the central sphere, the rightmost sphere is connected to the central sphere. The volume of the exclusion region is $v_1(D) = 2^d v_1(D/2)$.

indicator function is given by

$$f(\mathbf{r}) = \prod_{i=1}^{d} \Theta(D - |x_i|), \tag{8}$$

where $-\infty < x_i < \infty$ $(i = 1, 2, \ldots, d)$ denotes the ith Cartesian component of $\mathbf{r}$ and the coordinate system is chosen to align with the principal axes of the cubes. The volume of the cubical exclusion region $v_1(D)$ is again given by the volume integral of $f(\mathbf{r})$, i.e.,

$$v_1(D) = \int_{\mathbb{R}^d} f(\mathbf{r}) d\mathbf{r} = 2^d v_1(D/2), \tag{9}$$

where $v_1(D/2)$ is given by Eq. (3). Similarly, the mean number of overlaps per cube is still given by relation (7).

B. Cluster statistics and connectedness functions

The pair-connectedness function $P(\mathbf{r})$ is defined such that $\rho^2 P(\mathbf{r})\, d\mathbf{r}_1\, d\mathbf{r}_2$ is the probability finding any pair of particles of the same cluster in the volume elements $d\mathbf{r}_1$ and $d\mathbf{r}_2$ centered on $\mathbf{r}_1$ and $\mathbf{r}_2$, respectively, where $\mathbf{r} = \mathbf{r}_2 - \mathbf{r}_1$. We also consider the particle-averaged cluster number S (also referred to as the mean cluster size), which is the average number of particles in the cluster containing a randomly chosen particle. The mean cluster number S is given in terms of $P(\mathbf{r})$ for any statistically homogeneous system via a "compressibility-like" relation[6]

$$S = 1 + \rho \int_{\mathbb{R}^d} P(\mathbf{r})\, d\mathbf{r}. \tag{10}$$

The trivial first term of unity in this relation accounts for monomers, while the volume integral over $P(\mathbf{r})$ accounts for particle clustering (dimers, trimers, tetramers, etc.). Since $P(\mathbf{r})$ becomes long-ranged (i.e., decays to zero for large r slower than $1/r^d$) at the percolation threshold η_c, it follows from Eq. (10) that S diverges to infinity as $\eta \to \eta_c^-$. Indeed, it is believed that S obeys the power law,

$$S \propto (\eta_c - \eta)^{-\gamma}, \quad \eta \to \eta_c^-, \tag{11}$$

in the immediate vicinity of the percolation threshold. In this expression, γ is a universal exponent for a large class of lattice and continuum percolation models in dimension d, including not only spatially uncorrelated overlapping particles but also correlated continuum systems.[31] For example, $\gamma = 43/18$ for $d = 2$ and $\gamma = 1.8$ for $d = 3$ (see Refs. 2–4, and references therein). It is believed that when $d \geq d_c = 6$, where d_c is the "critical" dimension, the lattice- and continuum-percolation exponents take on their dimension-independent *mean-field* values,[2–4] which means in the case of (11) that $\gamma = 1$.

Coniglio *et al.*[6] derived the density expansion for the pair-connectedness function $P(\mathbf{r})$ in terms of the "Mayer-f" connectedness function, the latter of which characterizes the connectedness criterion. Specifically, $P(\mathbf{r})$ is identified as the collection of diagrams having at least one unbroken path of f-bonds connecting root points 1 and 2. The diagrams that constitute $P(\mathbf{r})$ can be divided into the *nodal* or *bridge* diagrams and the *non-nodal* or *direct* diagrams denoted by $C(\mathbf{r})$. The latter quantity is called the *direct connectedness function* and has the following density series expansion:

$$C(\mathbf{r}) = \sum_{n=2} \rho^{n-2} c_n(\mathbf{r}). \tag{12}$$

The first three terms of this series expansion have the following diagrammatic representations:

$c_2(\mathbf{r}) =$ 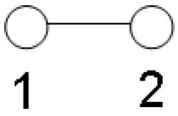 (13)

$\rho c_3(\mathbf{r}) =$ 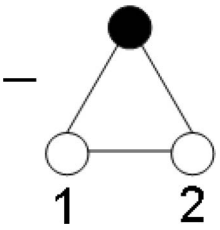 (14)

$\rho^2 c_4(\mathbf{r}) =$ 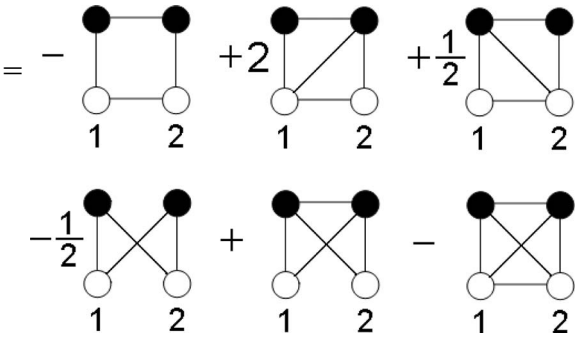 (15)

A diagram consists of a certain number of *circles* and f-bonds connecting the circles. There are two types of circles: white circles that are labeled and associated with the positions not integrated over (e.g., 1 and 2 in the expression given immediately above), and black circles associated with the integrated positions that are unlabeled, since they are dummy variables.

The aforementioned decomposition of the pair connectedness function into nodal and non-nodal diagrams results in an Ornstein–Zernike (OZ) relation, i.e.,

$$P(\mathbf{r}) = C(\mathbf{r}) + \rho C(\mathbf{r}) \otimes P(\mathbf{r}), \tag{16}$$

where $\otimes$ denotes a convolution integral. Taking the Fourier transform of Eq. (16) gives

$$\tilde{P}(\mathbf{k}) = \frac{\tilde{C}(\mathbf{k})}{1 - \rho \tilde{C}(\mathbf{k})}, \tag{17}$$

where $\mathbf{k}$ is the wave vector. Using the equivalent Fourier representation of the "compressibility" relation (10) for the mean cluster number S and Eq. (17), we arrive at

$$S = 1 + \rho \tilde{P}(0) = [1 - \rho \tilde{C}(0)]^{-1}. \tag{18}$$

The *direct* connectedness function $C(\mathbf{r})$ can immediately be used to determine the critical percolation density η_c. Since S diverges at the threshold, we have from Eq. (18) that

$$\eta_c = v_1(D/2)[\tilde{C}(0)]^{-1} = v_1(D/2)\left[\int C(\mathbf{r}) d\mathbf{r}\right]^{-1}. \tag{19}$$

The fact $\tilde{C}(0)$ is bounded at the percolation threshold implies that $C(\mathbf{r})$ is a short-ranged function, even at $\eta = \eta_c$, i.e., decays to zero for large $r \equiv |\mathbf{r}|$ faster than $1/r^d$ at the percolation threshold. These connectedness functions and related quantities have been analytically and numerically determined for overlapping spheres in one, two, and three dimensions.[7–13,15,16,18]

The density expansion of the mean cluster number,

$$S = 1 + \sum_{m=1} S_{m+1}\eta^m, \tag{20}$$

can be obtained from Eq. (18) and the series expansion,

$$\rho\tilde{C}(0) = \rho\int_{\mathbb{R}^d} C(\mathbf{r})d\mathbf{r} = \sum_{m=1} C_{m+1}\eta^m, \tag{21}$$

where

$$C_m = \frac{1}{v_1(D/2)^{m-1}}\int_{\mathbb{R}^d} c_m(\mathbf{r})d\mathbf{r} \tag{22}$$

and the functions $c_m(\mathbf{r})$ are defined by Eq. (12). One can easily verify that the coefficients S_m and C_m for $m \geq 2$ are related as follows:

$$S_m = \sum_{j=2}^{m} C_j S_{m+1-j}, \tag{23}$$

where $S_1 \equiv 1$. The first three inter-relations are given by

$$S_2 = C_2, \tag{24}$$

$$S_3 = C_2^2 + C_3, \tag{25}$$

$$S_4 = C_2^3 + 2C_2C_3 + C_4. \tag{26}$$

Using the definitions immediately above, we see that density expansion of the inverse mean cluster number S^{-1} is given by

$$S^{-1} = 1 - \rho\int_{\mathbb{R}^d} C(\mathbf{r})d\mathbf{r} = 1 - \sum_{m=1} C_{m+1}\eta^m. \tag{27}$$

It was once hypothesized that in the case of lattice percolation the percolation threshold or critical concentration corresponded to the radius of convergence of the series expansion for S. This hypothesis rested on the assumption that S had no singularities on the positive real axis for concentrations less than the critical value, i.e., the concentration coefficients (corresponding to the S_n in the continuum percolation problem) were all positive. It was shown that at sufficiently high order (e.g., 17th-order), the coefficients are sometimes negative for $d = 2$. This implies that the critical concentration does not correspond to the radius of convergence of the series expansion for S for $d = 2$, strongly suggesting that there is a closer singularity on the negative real axis.[32] Although no such an analogous results have been reported for the series expansion (20) due to the difficulty involved in ascertaining very high-order coefficients in low dimensions, we strongly expect that the convergence properties for continuum percolation to be qualitatively similar to that of Bernoulli lattice percolation, but only in sufficiently low dimensions when $d \geq 2$. Among other results, we show here that in sufficiently high dimensions, the radius of convergence of series expansion (20) corresponds to η_c.

It is well known that the integrals involved in computing the density expansion of the mean cluster number are the same as the ones that arise in the virial expansion of the hard-sphere or hard-cube system, even if the statistical weights are generally different from one another.[5] For example, the first two coefficients of the series expansion (21), i.e., the *dimer* and *trimer* contributions, are, respectively, given by

$$C_2 = \frac{1}{v_1(D/2)}\int_{\mathbb{R}^d} f(\mathbf{r})d\mathbf{r} = \frac{2B_2}{v_1(D/2)} = 2^d, \tag{28}$$

$$C_3 = -\frac{1}{v_1^2(D/2)}\int_{\mathbb{R}^d} f(\mathbf{r})v_2^{\text{int}}(\mathbf{r};D)d\mathbf{r} = -\frac{3\cdot B_3}{v_1(D/2)^2}, \tag{29}$$

where

$$v_2^{\text{int}}(\mathbf{r};D) = f(\mathbf{r}) \otimes f(\mathbf{r}) \tag{30}$$

is the intersection volume of two exclusion regions whose centroids are separated by the displacement vector $\mathbf{r}$. This exclusion region in the case of spheres and oriented cubes is a sphere of radius D and a cube of half-edge length D, respectively. The virial coefficient B_m is defined via the density expansion of the pressure p of a hard-particle system at number density ρ and temperature T, i.e.,

$$\frac{p}{\rho k_B T} = 1 + \sum_{m=1} B_{m+1}\rho^m. \tag{31}$$

The *tetramer* contribution to the series expansion (22) is also of direct interest in this paper. It can be simplified as follows:

$$C_4 = -\frac{3}{2}C_4^A + \frac{7}{2}C_4^B - C_4^C, \tag{32}$$

where

$$C_4^A = \frac{1}{v_1^3(D/2)}\int_{\mathbb{R}^d}\left[v_2^{\text{int}}(\mathbf{r};D)\right]^2 d\mathbf{r}, \tag{33}$$

$$C_4^B = \frac{1}{v_1^3(D/2)}\int_{\mathbb{R}^d} f(\mathbf{r})\left[v_2^{\text{int}}(\mathbf{r};D)\right]^2 d\mathbf{r}, \tag{34}$$

$$C_4^C = \frac{1}{v_1^3(D/2)}\int_{\mathbb{R}^d} f(\mathbf{r})\left[v_3^{\text{int}}(\mathbf{r}_{12},\mathbf{r}_{13},\mathbf{r}_{23};D)\right]^2 d\mathbf{r}, \tag{35}$$

and

$$v_3^{\text{int}}(\mathbf{r}_{12},\mathbf{r}_{13},\mathbf{r}_{23};D) = \int_{\mathbb{R}^d} f(\mathbf{r}_{14})f(\mathbf{r}_{24})f(\mathbf{r}_{34})d\mathbf{r}_4 \tag{36}$$

is the intersection volume of three exclusion regions whose centroids are separated by the displacement vectors $\mathbf{r}_{12}$, $\mathbf{r}_{13}$, and $\mathbf{r}_{23}$, respectively. The fourth virial coefficient B_4 for the corresponding hard-particle system is also obtained from the sum of the diagrams corresponding to C_4^A, C_4^B, and C_4^C but with the weights $-3/8$, $3/4$, and $-1/8$, respectively. Observe

that C_4^A is a four-particle "ring" diagram. While each of the diagrams C_4^A, C_4^B, and C_4^C are positive quantities, the entire tetramer statistic C_4 can be negative, which will be the case for sufficiently large d. Section III B shows that C_4 changes from a positive quantity to a negative quantity in relatively low dimensions for either hyperspheres or hypercubes.

C. Duality with the hard hyperspheres in equilibrium

Here, we show that the continuum percolation model of overlapping particles at number density ρ is in a particular sense *dual* to the corresponding hard-particle fluid system in equilibrium at number density ρ.[33] Of course, it must be kept in mind that the reduced density η for the percolation model is not the fraction of space covered by the particles, as it is in the hard-particle model.

First, we recall the well-known Ornstein-Zernike relation for a general one-component many-particle (not necessarily hard-particle) equilibrium system at number density ρ,

$$h(\mathbf{r}) = c(\mathbf{r}) + \rho c(\mathbf{r}) \otimes h(\mathbf{r}), \tag{37}$$

where $h(\mathbf{r}) = g_2(\mathbf{r}) - 1$ is the *total pair-correlation function*, $g_2(\mathbf{r})$ is the *pair-correlation function,* and $c(\mathbf{r})$ is the *direct correlation function*. We see that this is the analog of the percolation integral equation (16). The "compressibility relation" for general systems in equilibrium (hard particles or not) at number density ρ is exactly given by

$$\rho k_B T \kappa_T = 1 + \rho \int_{\mathbb{R}^d} h(r) d\mathbf{r}, \tag{38}$$

where k_B is Boltzmann's constant and $\kappa_T \equiv \frac{1}{\rho}(\frac{\partial \rho}{\partial p})_T$ is the isothermal compressibility.

For simplicity of discussion, we will specialize to the case of overlapping hyperspheres, keeping in mind that the generalization to overlapping hypercubes or other particle shapes is obvious. From the percolation OZ equation (16), the pair connectedness function $P(r)$ for overlapping hyperspheres of diameter D, exactly through first order in density, is

$$P(r) = f(r) + \rho[1 - f(r)]v_2^{\text{int}}(r; D) + \mathcal{O}(\rho^2). \tag{39}$$

Now we make the observation that this expansion for $P(r)$ is identical to $-h(r)$ for a hard-hypersphere system through the same order but evaluated at *negative density*; i.e., $P(r; \rho) = -h(r; -\rho)$ (see Hansen and MacDonald[34] for the hard-sphere diagrammatic expansion). Similarly, the direct connectedness function $C(r)$ through first order in ρ is identical to $-c(r)$ for a hard-hypersphere system through the same order but evaluated at *negative density*. This *duality* between these seemingly different physical problems at low densities applies as well in high dimensions for $\eta \leq \eta_c$, since we will see in Sec. IV that η_c tends to zero exponentially fast. Other manifestations of this duality are discussed further in Secs. V and IX.

III. TRIMER AND TETRAMER STATISTICS

A. Trimer statistics

The trimer contribution (29) to series expansion (21), which appears in relation (10) for the mean cluster number S, is of great importance in this paper. Since the trimer statistic (Eq. (29)) is the volume integral of the diagram given in Eq. (14), then it immediately follows that the absolute value of the ratio of the trimer statistic C_3 to the square of the dimer statistic (Eq. (28)) can be interpreted as a conditional probability. Specifically, given that particles 2 and 3 are each connected to particle 1, $|C_3|/C_2^2$ is the probability that the pair of particles 2 and 3 are connected to one another.

In what follows, we compute this conditional probability exactly as a function of dimension for both overlapping hyperspheres and overlapping oriented hypercubes. Importantly, we show that this probability vanishes as d becomes large, implying that trimers become more ramified or "branch-like." This is a consequence of the multitude of directions that become available for particles of a cluster to orient themselves with respect to one another as the dimension becomes large. Thus, ramification of finite clusters, i.e., k-mers with $k \geq 3$, is a general high-dimensional feature provided that $d \gg k$.

It is noteworthy that since the function $f(\mathbf{r})$ is unity inside an exclusion region and zero otherwise, it immediately follows that for any finite d, we have the following inequality for either overlapping hyperspheres or oriented hypercubes,

$$|C_3| < C_2^2 = 2^{2d}, \tag{40}$$

which in turn implies the positivity of $S_3 = C_2^2 + C_3$ for any finite d, i.e., $S_3 > 0$.

1. Hyperspheres

For hyperspheres, the integral that defines the trimer statistic (Eq. (29)) can be simplified as follows:

$$C_3 = -\frac{3 \cdot 2^{d-1} v_2^{\text{int}}(D; D)}{v_1(D/2)}. \tag{41}$$

We see that the trimer statistic is related to the intersection volume of two spherical exclusion regions of radius D. For hyperspheres, the situation is considerably more complicated than for oriented hypercubes, even if C_3/C_2^2 also tends to zero exponentially fast as $d \to \infty$, as we will show below. We denote by $\alpha(x; d) = v_2^{\text{int}}(x; R)/v_1(R)$ the volume common to two d-dimensional hyperspheres of radius R [in units of the volume of a sphere of radius R, $v_1(R)$] whose centers are separated by the dimensionless distance $x = r/(2R)$. We will call $\alpha(x; d)$ the *scaled intersection volume*, which will play an important role in this paper. The scaled intersection volume has the support [0, 1], the range [0, 1], and the following integral representation:[35]

$$\alpha(x; d) = c(d) \int_0^{\cos^{-1}(x)} \sin^d(\theta)\, d\theta, \tag{42}$$

where $c(d)$ is the d-dimensional constant given by

$$c(d) = \frac{2\Gamma(1 + d/2)}{\pi^{1/2}\Gamma[(d+1)/2]}. \tag{43}$$

We see from Eq. (41) that the trimer statistic $C_3(d)$ in dimension d is related to $\alpha(1/2; d)$, namely,

$$C_3(d) = -3 \cdot 2^{2d-1}\alpha(1/2; d). \tag{44}$$

Note that relation (42) for the scaled intersection volume for hyperspheres has been given explicitly in any space dimension in various representations.[35,36] For example, using

$$\alpha(x; 0) = \frac{2}{\pi}\cos^{-1}(x), \quad \alpha(x; 1) = 1 - x$$

and the recursive relation,

$$\alpha(x; d) = \alpha(x; d-2) - \frac{\Gamma(d/2)}{\sqrt{\pi}\Gamma((d+1)/2)}x(1-x^2)^{\frac{d-1}{2}}, \quad d \geq 2, \tag{45}$$

obtained by integrating Eq. (42) by parts, yields the scaled intersection volume for any $d \geq 2$. For example, for $d = 2, 3, 4$, and 5, we have, for $x \leq 1$, that

$$\alpha(x; 2) = \frac{2}{\pi}\left[\cos^{-1}(x) - x(1-x^2)^{1/2}\right], \tag{46}$$

$$\alpha(x; 3) = 1 - \frac{3}{2}x + \frac{1}{2}x^3, \tag{47}$$

$$\alpha(x; 4) = \frac{2}{\pi}\left[\cos^{-1}(x) - \left\{\frac{5x}{3} - \frac{3}{4}x^3\right\}(1-x^2)^{1/2}\right], \tag{48}$$

$$\alpha(x; 5) = 1 - \frac{15}{8}x + \frac{5}{4}x^3 - \frac{3}{8}x^5. \tag{49}$$

Torquato and Stillinger[35] found the following series representation of the scaled intersection volume $\alpha(x; d)$ for $x \leq 1$ and any d:

$$\alpha(r; R) = 1 - c(d)x + c(d)\sum_{n=2}^{\infty}(-1)^n \times \frac{(d-1)(d-3)\cdots(d-2n+3)}{(2n-1)[2\cdot 4\cdot 6\cdots(2n-2)]}x^{2n-1}. \tag{50}$$

For even dimensions, relation (50) is an infinite series, but for odd dimensions, the series truncates such that $\alpha(x; d)$ is a univariate polynomial of degree d.

Figure 4 shows graphs of the scaled intersection volume $\alpha(x; d)$ as a function of x for the first five space dimensions. For any dimension, $\alpha(x; d)$ is a monotonically decreasing function of x. At a fixed value of x in the open interval $(0, 1)$, $\alpha(x; d)$ is a monotonically decreasing function of the dimension d.

Using the definition (44) and the recursive relation (45) yields the corresponding recursive relation for the trimer statistic,

$$C_3(d) = 16 \cdot C_3(d-2) + \frac{3\cdot 2^{2d-2}\,\Gamma(d/2)}{\sqrt{\pi}\Gamma((d+1)/2)}\left(\frac{3}{4}\right)^{\frac{d-1}{2}}, \quad d \geq 2, \tag{51}$$

where $C_3(0) = -1$ and $C_3(1) = -3$. Table I lists the conditional trimer probability $|C_3|/C_2^2 = -C_3/C_2^2$ (discussed earlier) for the first 11 space dimensions. This table indicates that the ratio $|C_3|/C_2^2$ monotonically decreases as d increases, presumably tending to zero. Indeed, this is the case. For large d,

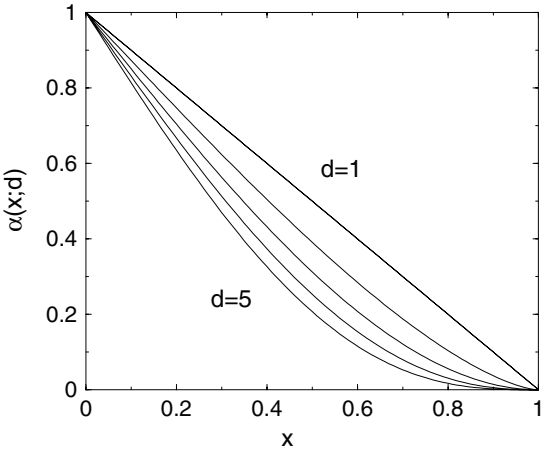

FIG. 4. The scaled intersection volume $\alpha(x; d)$ for spherical windows of radius 1/2 as a function of x for the first five space dimensions. The uppermost curve is for $d = 1$ and lowermost curve is for $d = 5$.

we will make use of the leading-order asymptotic result,[35]

$$C_3(d) \sim -\left(\frac{6}{\pi d}\right)^{1/2} 2^{d-1}\cdot 3^{\frac{d+2}{2}}. \tag{52}$$

Thus, the conditional probability $|C_3|/C_2^2$ goes to zero exponentially fast as $d \to \infty$, since

$$\frac{|C_3|}{C_2^2} \sim \left(\frac{24}{\pi d}\right)^{1/2}\left(\frac{3}{4}\right)^{\frac{d+2}{2}}, \quad d \to \infty. \tag{53}$$

2. Hypercubes

Evaluations of the terms in the density expansion of S for overlapping oriented hypercubes are considerably easier than those for overlapping hyperspheres since individual diagrams

TABLE I. Conditional trimer probability $|C_3|/C_2^2 = -C_3/C_2^2$ for overlapping hyperspheres, denoted by $(|C_3|/C_2^2)_{\text{sphere}}$ and overlapping oriented hypercubes, denoted by $(|C_3|/C_2^2)_{\text{cube}}$, for dimensions one through eleven.

d	$(\lvert C_3\rvert/C_2^2)_{\text{sphere}}$	$(\lvert C_3\rvert/C_2^2)_{\text{cube}}$
1	$\frac{3}{4} = 0.7500000000\ldots$	$\frac{3}{4} = 0.7500000000\ldots$
2	$1 - \frac{3\sqrt{3}}{4\pi} = 0.5865033288\ldots$	$\left(\frac{3}{4}\right)^2 = 0.5625000000\ldots$
3	$\frac{15}{32} = 0.4687500000\ldots$	$\left(\frac{3}{4}\right)^3 = 0.4218750000\ldots$
4	$1 - \frac{9\sqrt{3}}{9\pi} = 0.3797549926\ldots$	$\left(\frac{3}{4}\right)^4 = 0.3164062500\ldots$
5	$\frac{159}{512} = 0.3105468750\ldots$	$\left(\frac{3}{4}\right)^5 = 0.2373046875\ldots$
6	$1 - \frac{27\sqrt{3}}{20\pi} = 0.2557059910\ldots$	$\left(\frac{3}{4}\right)^6 = 0.1779785156\ldots$
7	$\frac{867}{4096} = 0.2116699219\ldots$	$\left(\frac{3}{4}\right)^7 = 0.1334838867\ldots$
8	$1 - \frac{837\sqrt{3}}{560\pi} = 0.1759602045\ldots$	$\left(\frac{3}{4}\right)^8 = 0.1001129150\ldots$
9	$\frac{19239}{131072} = 0.1467819214\ldots$	$\left(\frac{3}{4}\right)^9 = 0.07508468628\ldots$
10	$1 - \frac{891\sqrt{3}}{560\pi} = 0.1227963465\ldots$	$\left(\frac{3}{4}\right)^{10} = 0.05631351471\ldots$
11	$\frac{107985}{1048576} = 0.1029825211\ldots$	$\left(\frac{3}{4}\right)^{11} = 0.04223513603\ldots$

for the former in any dimension d can be expressed as the one-dimensional solution raised to the power d. For example, for one-dimensional "cubes" of length D, the intersection volume of two such cubes (i.e., line intervals) as a function of the displacement vector $\mathbf{r}$ between their centroids is given by

$$v_2^{\text{int}}(|\mathbf{r}|; D) = 2D\left[1 - \frac{|\mathbf{r}|}{2D}\right]\Theta(2D - |\mathbf{r}|). \tag{54}$$

Thus, the trimer statistic (Eq. (29)) for overlapping oriented hypercubes in dimension d is

$$C_3(d) = -|C_3(1)|^d = -3^d, \tag{55}$$

where the one-dimensional trimer statistic $C_3(1)$, defined by Eq. (29), is

$$C_3(1) = -\frac{4}{D^2}\int_0^D v_2^{\text{int}}(x; D)dx = -3\,. \tag{56}$$

Therefore, the conditional trimer probability for any d is exactly given by

$$\frac{|C_3|}{C_2^2} = \left(\frac{3}{4}\right)^d, \tag{57}$$

which we see tends to zero exponentially fast as $d \to \infty$.

B. Tetramer statistics

Because $f(\mathbf{r})$ is a unit-step function, the ring diagram C_4^A in the tetramer statistic (Eq. (32)) is always greater than either C_4^B or $C_4^C < C_4^B$, but always smaller than $2^d|C_3|$ for finite d for either hypersphere or hypercubes, i.e.,

$$C_4^C < C_4^B < C_4^A < 2^d|C_3|\,. \tag{58}$$

We will see below that the absolute value of the tetramer statistic C_4 is bounded from above by

$$|C_4| < 2^d|C_3|. \tag{59}$$

1. Hyperspheres

To evaluate the tetramer statistic C_4 [cf. Eq. (32)] for overlapping hyperspheres for the first 11 dimensions, the ring diagram C_4^A contribution as well as that from the diagram C_4^B can be directly determined using the scaled intersection volume $\alpha(x; d)$ obtained from the recurrence relation (45). To evaluate the remaining "star" diagram contribution C_4^C to C_4, we utilize results for the "star" diagram contribution to the fourth virial coefficient B_4 for hard hyperspheres obtained in two and three dimensions[37,38] as well as in higher dimensions[39,40] as per the discussion at the end of Sec. II. Table II lists the scaled tetramer statistic C_4/C_2^3 for overlapping hyperspheres for the first 11 space dimensions. This table indicates that the ratio $|C_4|/C_2^3$ is always smaller than unity and is a monotonically decreasing function of d, presumably tending to zero. Comparing these results for hyperspheres to Table I, we see that inequality (59) relating the tetramer statistic C_4 to the trimer statistic C_3 is obeyed.

Not only is the ring diagram C_4^A larger than either of the other diagrams C_4^B and C_4^C that contributes to C_4 for any finite d, as noted at the end of Sec. II, but C_4^B and C_4^C become subdominant compared to C_4^A in the large-d limit, i.e.,

$$\frac{C_4^B}{C_4^A} \to 0, \quad \frac{C_4^C}{C_4^A} \to 0, \quad \text{as} \quad d \to \infty. \tag{60}$$

This is a well-known property of not only this ring diagram but all higher order ring diagrams in the context of hard hyperspheres.[41] Thus, for some sufficiently large critical dimension, the ring diagram contribution to C_4 becomes appreciably larger than the other contributions, implying that tetramer statistic C_4 must change from a positive quantity below this critical dimension to a negative quantity at and above this critical dimension (since the ring-diagram contribution is weighted with a minus sign). Indeed, we see from Table II that this critical dimension is 11. Note also that the scaled tetramer statistic C_4/C_2^3 or C_4^A/C_2^3 tends to zero in the high-d limit according to the following leading-order asymptotic behavior:

$$\frac{C_4}{C_2^3} \to -\frac{3}{2}\frac{C_4^A}{C_2^3} \sim -\left(\frac{24}{\pi d}\right)^{1/2}\left(\frac{4}{3\sqrt{3}}\right)^d, \quad d \to \infty. \tag{61}$$

Combination of the asymptotic formulas (53) and (61) yields that the ratio $|C_4|/(2^d|C_3|)$ goes to zero exponentially fast in the high-dimensional limit according to the relation

$$\frac{|C_4|}{2^d|C_3|} \sim \frac{4}{3}\left(\frac{8}{9}\right)^d, \quad d \to \infty. \tag{62}$$

2. Hypercubes

Again, since the individual diagrams involved in the tetramer statistic (Eq. (32)) for overlapping oriented hypercubes in any dimension d can be expressed as the one-dimensional solution raised to the power d, we find that $C_4^A = 2^{3d}(2/3)^d$, $C_4^B = (14/3)^d$, and $C_4^C = 4^d$. Therefore, from Eq. (32), the tetramer statistic is given by

$$C_4 = -2^{3d}\left(\frac{2}{3}\right)^{d-1} + \frac{7}{2}\left(\frac{14}{3}\right)^d - 4^d. \tag{63}$$

TABLE II. Scaled tetramer statistic C_4/C_2^3 for overlapping hyperspheres, denoted by $(C_4/C_2^3)_{\text{sphere}}$ and overlapping oriented hypercubes, denoted by $(C_4/C_2^3)_{\text{cube}}$, for dimensions one through eleven.

d	$(C_4/C_2^3)_{\text{sphere}}$	$(C_4/C_2^3)_{\text{cube}}$
1	0.5416666667	$\frac{13}{24} = 0.5416666667$
2	0.3110703762	$\frac{79}{288} = 0.2743055556$
3	0.1823550119	$\frac{433}{3456} = 0.1252893519$
4	0.1070948907	$\frac{1927}{41\,472} = 0.04646508488$
5	0.06210757652	$\frac{3793}{497\,664} = 0.007621608153$
6	0.03498939854	$-\frac{56\,201}{5\,971\,968} = -0.009410800594$
7	0.01866770530	$-\frac{1\,086\,527}{71\,663\,616} = -0.01516148725$
8	0.008950018335	$-\frac{13\,337\,273}{859\,963\,392} = -0.01550911716$
9	0.003289929140	$-\frac{140\,333\,327}{10\,319\,560\,704} = -0.01359876947$
10	0.0001175430431	$-\frac{1\,364\,831\,081}{123\,834\,728\,448} = -0.01102139196$
11	−0.001543006376	$-\frac{12\,654\,110\,687}{1\,048\,576} = -0.006371786923$

In the limit that $d \to \infty$, the ratio $|C_4|/C_2^3$ goes to zero exponentially fast according to

$$\frac{|C_4|}{C_2^3} \sim \left(\frac{2}{3}\right)^d. \tag{64}$$

Combination of the asymptotic formulas (57) and (64) gives that the ratio $|C_4|/(2^d|C_3|)$ goes to zero exponentially fast in the high-dimensional limit according to the asymptotic relation

$$\frac{|C_4|}{2^d|C_3|} \sim \left(\frac{8}{9}\right)^d, \quad d \to \infty. \tag{65}$$

C. Higher-order statistics in the high-dimensional limit

It is useful for later purposes to bound the successive coefficients C_k and C_{k+1} for large dimensions. In particular, we have that

$$|C_k| > \frac{|C_{k+1}|}{C_2} = \frac{|C_{k+1}|}{2^d}, \quad \text{for } k \geq 2 \text{ and } d \gg 1. \tag{66}$$

This inequality follows because the ring-diagram contribution to C_k dominants among all others because $f(\mathbf{r})$ is a unit step function. The bound indicated in relation (66) likely applies in all dimensions, e.g., we have shown above that it is valid when $k = 2$ and 3 for any d. One can easily verify, using the results of Sec. VI A, that it is also valid in one dimension for any k.

IV. EXACT HIGH-*d* ASYMPTOTICS FOR PERCOLATION BEHAVIOR

On physical grounds, it is clear that the threshold η_c for either overlapping hyperspheres or hypercubes must tend to zero as d tends to infinity. Indeed, we now show that in sufficiently high dimensions, the threshold η_c has the following exact asymptotic expansion:

$$\eta_c = \frac{1}{2^d} - \frac{C_3}{2^{3d}} - \frac{C_4}{2^{4d}} + \mathcal{O}\left(\frac{C_3^2}{2^{5d}}\right), \quad d \gg 1. \tag{67}$$

The terms in this expansion are written in order of decreasing dominance. Thus, using this relation in the expression (7) yields the corresponding asymptotic expansion for mean number of overlaps per particle $\mathcal{N}_c$ at the threshold, i.e.,

$$\mathcal{N}_c = 1 - \frac{C_3}{2^{2d}} - \frac{C_4}{2^{3d}} + \mathcal{O}\left(\frac{C_3^2}{2^{4d}}\right), \quad d \gg 1. \tag{68}$$

Hence, in the infinite-dimensional limit, we exactly have

$$\eta_c \sim \frac{1}{2^d}, \quad d \to \infty, \tag{69}$$

$$\mathcal{N}_c \sim 1, \quad d \to \infty, \tag{70}$$

where we have used the asymptotic results for C_3 and C_4 obtained in Sec. III. We see that η_c tends to zero exponentially fast as $d \to \infty$ and each sphere overlaps exactly one other sphere on average in this asymptotic limit. The latter result is the theoretical basis for the same numerical observation reported by Krüger.[29]

To obtain the asymptotic relation (Eq. (67)) for the percolation threshold η_c, it is important to recognize that the sum of the first few terms in the exact expression (Eq. (27)) for S^{-1}, which is a low-degree polynomial in η, is sufficient to determine η_c in high dimensions. Specifically, η_c is the relevant zero of this low-degree polynomial in η. We illustrate this idea by showing how to obtain the leading-order term in Eq. (67), i.e., $1/2^d$. Let us rewrite the exact expression for the inverse of the mean cluster number as follows:

$$S^{-1} = 1 - 2^d\eta - R_2(\eta), \tag{71}$$

where

$$R_n(\eta) = \sum_{m=n}^{\infty} C_{m+1}\eta^m \tag{72}$$

is the nth-order remainder of the series expansion (21) for $\rho\tilde{C}(0)$. Now if we can show that the remainder $R_2(\eta = 1/2^d)$ tends to zero as d tends to infinity, then the proof would be complete, since $\eta = 1/2^d$ is trivially the zero of $1 - 2^d\eta$. Since

$$R_2(\eta = 1/2^d) = \frac{C_3}{2^{2d}} + \frac{C_4}{2^{3d}} + \cdots, \tag{73}$$

it immediately follows from the asymptotic results obtained in Sec. III that

$$\lim_{d\to\infty} R_2(\eta = 1/2^d) \to 0, \tag{74}$$

which completes the proof. This analysis implies that

$$S \sim \frac{1}{1 - 2^d\eta}, \quad d \to \infty, \tag{75}$$

and thus the asymptotic relation (Eq. (69)) for the percolation threshold η_c. We will see in Sec. VI B that expression (75) is a rigorous upper bound on the mean cluster number for any dimension d and reduced densities in the interval $[0, 2^{-d}]$.

Now to obtain the next terms in the asymptotic expansion (67), successively more terms are included in the partial sum (e.g., quadratic and cubic terms in η) and its roots are determined. One can again show that the remainder $R_4(\eta)$ when evaluated at $\eta = 1/2^d - C_3/2^{3d} - C_4/2^{4d}$ tends to zero as d tends to infinity.

V. PERCUS-YEVICK APPROXIMATION FOR CLUSTER STATISTICS

Stell[8] has shown a remarkable correspondence between the Percus-Yevick (PY) approximations for the pair connectedness function $P(r)$ for overlapping particles and the pair correlation function of hard spheres continued analytically to $-\rho$. This is another manifestation of the duality between the two problems described in Sec. II C that applies in all dimensions, albeit approximately. The PY approximation for hard hyperspheres of diameter D solves the OZ equation (37) assuming the closure

$$c(r) = 0 \quad \text{for} \quad r > D, \quad h(r) = -1 \quad \text{for} \quad r < D. \tag{76}$$

The analogous PY closure for the percolation OZ equation (16) is specified by

$$C(r) = 0 \quad \text{for} \quad r > D, \quad P(r) = 1 \quad \text{for} \quad r < D. \tag{77}$$

Therefore, comparison of the two different integral equations (16) and (37) with their corresponding PY closures reveals that $P(r)$ and $C(r)$ at ρ can be mapped to $-h(r)$ and $-c(r)$ at $-\rho$, respectively. Since the PY approximation is exact up through the third virial coefficient, this implies that it yields the direct connectedness function $C(r)$ in Eq. (12) exactly up through first order in density or, equivalently, expansion (39) for $P(r)$.

A consequence of this correspondence is that the mean cluster number S for overlapping particles, which is exactly given by Eq. (10), can be obtained within the PY approximation from the corresponding hard-particle solution of the compressibility relation (38), i.e.,

$$S = k_B T \left(\frac{\partial \rho}{\partial p}\right)_{\rho \to -\rho} = 1 - \rho \int_{\mathbb{R}^d} h(r; -\rho) d\mathbf{r}, \tag{78}$$

where $h(r; -\rho)$ indicates the total correlation function evaluated at $-\rho$. Since the PY approximation is exact up through the third virial level, the mean cluster size for overlapping particles within the PY approximation is exact up through the second order in ρ or η, i.e., it yields the exact series coefficients S_2 and S_3 defined in Eq. (20) or, equivalently, the exact coefficients C_2 and C_3 defined by Eqs. (28) and (29), respectively.

Using this prescription and the Percus-Yevick-like expression for the pressure for a d-dimensional hard-sphere or oriented hard-cube derived in Appendix A, we arrive at the following PY-like expression for S for overlapping hyperspheres or oriented hypercubes,

$$S \approx S^{\text{PY}} = \frac{(1+\eta)^{d+1}}{1 + A_1\eta + A_2\eta^2 + A_3\eta^3}, \tag{79}$$

where

$$A_1 = d + 1 - C_2, \tag{80}$$

$$A_2 = \frac{d(d+1)}{2} - \frac{(d+1)C_2}{2} - C_3, \tag{81}$$

$$A_3 = (3-d)\left[\frac{d(d-1)}{2} - \frac{C_2 d}{2} - \frac{C_3}{3}\right]. \tag{82}$$

Thus, the predicted percolation threshold is obtained by finding the appropriate zero η_0^{PY} of the cubic polynomial in the denominator of Eq. (79). Thus, in this approximation,

$$\eta_c \approx \eta_0^{\text{PY}}. \tag{83}$$

The root η_0^{PY} is meaningful for $d \geq 3$. Expanding the inverse of Eq. (79) through order η^3 yields

$$S^{-1} \approx (S^{\text{PY}})^{-1} = 1 - C_2\eta - C_3\eta^2 + \left[\frac{4d}{3}C_3 + d(d-1)C_2 - \frac{2d(d-2)(d-1)}{3}\right]\eta^3 + \mathcal{O}(\eta^4). \tag{84}$$

Thus, since this approximation is exact through second order in η [cf. Eq. (21)], we see that the tetramer coefficient within this approximation is given by

$$C_4 \approx -\frac{4d}{3}C_3 - d(d-1)C_2 + \frac{2d(d-2)(d-1)}{3}. \tag{85}$$

For sufficiently large d, the cubic term in the denominator can be neglected, and hence, estimate of η_c is given by the appropriate root of the remaining quadratic relation, i.e.,

$$\eta_0^{\text{PY}} \approx \frac{(d+1) - C_2 + \sqrt{(1+C_2)^2 + 2d(C_2 - d) + 4C_3}}{2C_2(d+1) - d(d+1) + 2C_3}. \tag{86}$$

This high-dimensional quadratic solution matches the exact cubic solution to at least three significant figures in eight dimensions, a relatively low dimension. Finally, we note that Eq. (86) asymptotically becomes

$$\eta_0^{\text{PY}} \sim \frac{1}{2^d} - \frac{C_3}{2^{3d}} - \frac{d}{2^{2d}} + \quad \text{h.o.t} \quad (d \gg 1), \tag{87}$$

which is the exact form up through the first two terms [cf. Eq. (67)], since this approximation is exact through the third virial level. Note we have used Eq. (28), i.e., $C_2 = 2^d$.

VI. LOWER BOUNDS ON THE PERCOLATION THRESHOLD

It has been observed that the $[n, 1]$ Padé approximant of the mean cluster number S provides lower bounds on η_c for overlapping spheres in two and three dimensions (as determined by numerical simulations) and become sharper as n increases, where $n = 0, 1, 2, \ldots$.[19] Let us denote the $[n, 1]$ Padé approximant of the mean cluster number S by $S_{[n,1]}$. This rational function for any d is given explicitly by

$$S \approx S_{[n,1]} = \frac{1 + \sum_{m=1}^{n}\left[S_{m+1} - S_m \frac{S_{n+2}}{S_{n+1}}\right]\eta^m}{1 - \frac{S_{n+2}}{S_{n+1}}\eta}, \quad \text{for} \quad 0 \leq \eta \leq \eta_0^{(n)}, \tag{88}$$

where $\eta_0^{(n)}$ is the pole of the $[n, 1]$ approximant, which is given by

$$\eta_0^{(n)} = \frac{S_{n+1}}{S_{n+2}}, \quad \text{for} \quad n \geq 0. \tag{89}$$

Here we use the convention that the sum in Eq. (88) is zero in the single instance in which $n = 0$. The claim we make is that the pole $\eta_0^{(n)}$ for $n = 0$, 1, and 2 bounds the threshold η_c from below for any d, i.e.,

$$\eta_c \geq \eta_0^{(n)} = \frac{S_{n+1}}{S_{n+2}}, \quad \text{for} \quad n = 0,\ 1,\ 2, \tag{90}$$

and hence,

$$\mathcal{N}_c \geq 2^d \frac{S_{n+1}}{S_{n+2}}, \quad \text{for} \quad n = 0,\ 1,\ 2. \tag{91}$$

A. Proof in the one-dimensional case

For $d = 1$, it is simple to show that all $[n, 1]$ Padé approximants of S ($n = 0, 1, 2, 3, \ldots$) provide lower bounds on the percolation threshold. To see this, note the mean cluster number S in the one-dimensional case is given exactly by

$$S = \frac{1+\phi}{1-\phi}, \tag{92}$$

where $\phi = 1 - e^{-\eta}$ is the fraction of space covered the overlapping particles.[19] Thus, the mean cluster number can be written as

$$S = 2e^{\eta} - 1 = 1 + \sum_{k=1}^{\infty} \frac{2}{k!}\eta^k. \tag{93}$$

Comparing this relation to Eq. (20) yields

$$S_m = \frac{2}{(m-1)!}, \quad \text{for} \quad m \geq 2. \tag{94}$$

We see from Eq. (89) that

$$\eta_0^{(n)} = n + 2, \tag{95}$$

and hence, this pole always bounds the actual percolation threshold $\phi_1 = 1$ [cf. Eq. (92)] or $\eta_c = \infty$ from below:

$$\eta_c \geq n + 2, \quad \text{for} \quad n \geq 0. \tag{96}$$

Note that the lower bound (96) progressively becomes tighter as the order of the $[n, 1]$ Padé approximant of S increases. Apparently, as we will see below, these lower bound properties of the $[n, 1]$ Padé approximant of S extend to all dimensions for sufficiently small n.

B. [0, 1] Padé approximant

We will begin by proving that the $[0, 1]$ Padé approximant of the mean cluster number S given by

$$S \approx S_{[0,1]} = \frac{1}{1 - 2^d\eta}, \quad \text{for} \quad 0 \leq \eta \leq \frac{1}{2^d}, \tag{97}$$

provides the following rigorous lower bound on the percolation threshold η_c in all Euclidean dimensions,

$$\eta_c \geq \eta_0^{(0)} = \frac{1}{2^d}. \tag{98}$$

This in turn directly implies the lower bound

$$\mathcal{N}_c \geq 1. \tag{99}$$

Given and Stell[15] derived bounds on the pair connectedness function for overlapping spheres, which trivially take the following more general form for anisotropic particle shapes:

$$P(\mathbf{r}) \geq f(\mathbf{r}), \tag{100}$$

$$P(\mathbf{r}) \leq f(\mathbf{r}) + \rho[1 - f(\mathbf{r})]f(\mathbf{r}) \otimes P(\mathbf{r}). \tag{101}$$

Note that since $1 - f(\mathbf{r}) \leq 1$, we also have from the inequality (101), the weaker upper bound

$$P(\mathbf{r}) \leq f(\mathbf{r}) + \rho f(\mathbf{r}) \otimes P(\mathbf{r}). \tag{102}$$

Taking the volume integral of Eq. (102) and using the definition (10) for the mean cluster number S yields the following upper bound on the latter:

$$S \leq \frac{1}{1 - S_2\eta}. \tag{103}$$

Now since this lower bound has a pole at $\eta = S_2^{-1} = C_2^{-1}$, it immediately implies the new rigorous lower bound (98) on the percolation threshold for any d.[42] This in turn implies the following rigorous lower bound on the mean number of overlaps per particle $\mathcal{N}_c$ at the threshold for any d:

$$\mathcal{N}_c \geq 1. \tag{104}$$

This rigorous lower bound contradicts the numerical results reported in Ref. 30 that $\mathcal{N}_c$ is less than unity for hyperspheres in high dimensions.

Note that the lower bound (100) and upper bound (101) imply that in the limit $d \to \infty$,

$$P(\mathbf{r}) \to f(\mathbf{r}), \quad \text{for} \quad 0 \leq \eta \leq \frac{1}{2^d}. \tag{105}$$

This follows since the higher terms in the upper bound (101) vanish in the limit $d \to \infty$ in light of the asymptotic properties established above. Thus, for overlapping hyperspheres, this result means that $P(r)$ tends to a step function, i.e.,

$$P(\mathbf{r}) \to \Theta(D - r), \quad \text{for} \quad 0 \leq \eta \leq \frac{1}{2^d}. \tag{106}$$

The dual statement for the hard-hypersphere correlation function is described in Sec. IX.

Note that a stronger upper bound on $P(\mathbf{r})$ can be obtained by using the lower bound (100) in the inequality (101), namely,

$$P(\mathbf{r}) \leq f(\mathbf{r}) + \rho f(\mathbf{r}) \otimes P(\mathbf{r}) - \rho f(\mathbf{r})[f(\mathbf{r}) \otimes P(\mathbf{r})]. \tag{107}$$

Taking the volume integral of Eq. (102) and use of Eq. (10) gives the following upper bound:

$$S \leq \frac{1 - C_3\eta^2}{1 - S_2\eta}. \tag{108}$$

Although this lower bound on S is sharper than inequality (103), it has the same pole and, therefore, does not provide a tighter upper bound on the percolation threshold than inequality (98).

It is instructive to analyze the implications of the upper bound (103) or lower bound on S^{-1}. In particular, using relations (27) and (103), we have that

$$1 - 2^d\eta \leq S^{-1} = 1 - 2^d\eta - R_2(\eta), \quad 0 \leq \eta \leq \frac{1}{2^d}, \tag{109}$$

where $R_2(\eta)$ is the second-order remainder defined by Eq. (72) with $n = 2$. Therefore, the remainder $R_2(\eta)$ is negative semi-definite, i.e.,

$$R_2(\eta) \leq 0, \tag{110}$$

which is tantamount to saying that the left side of inequality (109) bounds S^{-1} from below. This remainder property is

true for $\eta = 1/2^d$, and hence, its density expansion obeys the inequality

$$R_2(\eta = 2^{-d}) = \frac{C_3}{2^{2d}} + \frac{C_4}{2^{3d}} + \mathcal{O}\left(\frac{C_5}{2^{4d}}\right) \geq 0. \tag{111}$$

The sign of the first term in this sum is negative and determines the sign of the entire sum.

C. [1, 1] Padé approximant

The [1, 1] Padé approximant of S, given by Eq. (88) with $n = 1$, is more explicitly given by

$$S \leq S_{[1,1]} = \frac{1 + \left[2^d - \frac{S_3}{2^d}\right]\eta}{1 - \frac{S_3}{2^d}\eta}, \quad \text{for} \quad 0 \leq \eta \leq \eta_0^{(1)}, \tag{112}$$

provides the following putative lower bound on the threshold η_c in all Euclidean dimensions:

$$\eta_c \geq \eta_0^{(1)} = \frac{1}{2^d\left[1 + \frac{C_3}{2^{2d}}\right]}, \tag{113}$$

where $\eta_0^{(1)}$ is the pole defined by Eq. (89) and we have made use of the identities (24) and (25) with $S_2 = C_2 = 2^d$. We see that since C_3 is negative, this putative lower bound improves upon the lower bound (98) obtained from the [0, 1] Padé approximant for any finite d.

We now examine whether relation (113) is indeed a rigorous lower bound on η_c or, equivalently, relation (112) is an upper bound on S, which provides a lower bound on S^{-1}. The bounds (100) and (101) on the connectedness function, unlike the case of the [0, 1] Padé approximant, do not contain sufficient information to prove that relation (113) is a lower bound. Therefore, we must use a different approach. Note that $S^{-1}_{[1,1]}$ can be written as

$$S^{-1}_{[1,1]} = 1 - 2^d\eta - C_3\eta^2 - \sum_{k=3} \frac{C_3^{k-1}}{2^{d(n-2)}}\eta^k. \tag{114}$$

Thus, for this expression to bound S^{-1} from below, it is required that the difference $R_3(\eta) - S^{-1}_{[1,1]}$ be negative or

$$\left[C_4 - \frac{C_3^2}{2^d}\right] + \left[C_5 - \frac{C_3^3}{2^{2d}}\right]\eta + \left[C_6 - \frac{C_3^4}{2^{3d}}\right]\eta^2 + \text{ h.o.t} \leq 0,$$
$$\text{for} \quad 0 \leq \eta \leq \eta_0^{(1)}. \tag{115}$$

First, we observe that the first bracketed term is negative, which follows immediately from the results of Sec. III. Therefore, for sufficiently small η, the inequality (115) must be obeyed, since all terms after the first bracketed term are subdominant. Second, for sufficiently large d, again the inequality (115) must be obeyed because

$$\left|C_4 - \frac{C_3^2}{2^d}\right| \geq \left|C_k - \frac{C_3^{k-2}}{2^{d(k-3)}}\right|\eta_0^{(k-4)}, \quad \text{for all } k \geq 5, \tag{116}$$

and the ratio of the right side to the left side of this inequality tends to zero as $d \to \infty$. Here, we have again used the results of Sec. III, including inequality (66), which results from the fact that the ring-diagram contributions to C_k dominant in the large-d limit. These results combined with the fact relations (112) and (113) are indeed rigorous upper and lower bounds on S and η_c, respectively, for $d = 1$ (Sec. VI A) provide strong theoretical arguments that these are rigorous bounds for all dimensions. Moreover, we will also see that numerical simulations in sufficiently low dimensions support these claims.

Note that for large d, the pole $\eta_0^{(1)}$ has the following asymptotic behavior:

$$\eta_0^{(1)} = \frac{1}{2^d} - \frac{C_3}{2^{3d}} + \frac{C_3^2}{2^{5d}} + \mathcal{O}\left(\frac{C_3^3}{2^{7d}}\right), \quad d \gg 1 \tag{117}$$

Notice that the first two terms in this expression match the exact asymptotic expansion (87). Since $|C_3|/2^{2d}$ tends to zero exponentially fast as $d \to \infty$ for both hyperspheres and hypercubes [cf. Eqs. (53) and (57)], the lower bound (113) tends to the exact asymptotic result of $1/2^d$ in this limit [cf. Eq. (69)] for these models.

D. [2, 1] Padé approximant

The [2, 1] Padé approximant of the mean cluster number S, given by Eq. (88) with $n = 2$, is more explicitly given by

$$S \leq S_{[1,1]} = \frac{1 + \left[2^d - \frac{S_4}{S_3}\right]\eta + \left[S_3 - \frac{2^d S_4}{S_3}\right]\eta^2}{1 - \frac{S_4}{S_3}\eta},$$
$$\text{for} \quad 0 \leq \eta \leq \eta_0^{(2)}, \tag{118}$$

provides the following putative lower bound on the percolation threshold η_c in all d:

$$\eta_c \geq \eta_0^{(2)} = \frac{1 + \frac{C_3}{2^{2d}}}{2^d\left[1 + \frac{2C_3}{2^{2d}} + \frac{C_4}{2^{3d}}\right]}, \tag{119}$$

where $\eta_0^{(2)}$ is the pole defined by Eq. (89) and we have made use of the identities (24)–(26) with $S_2 = C_2 = 2^d$. Observe that because of the properties of C_3 and C_4 discussed in Sec. III, the putative lower bound (119) improves upon the lower bound (113) arising from the [1, 1] Padé approximant for any finite d.

Using the same analysis described above for the [1, 1] Padé approximant, it is simple to show that relation (118) is an upper bound on S for sufficiently small η and sufficiently large d for $0 \leq \eta \leq \eta_0^{(2)}$, which implies the lower bound (119) at least for sufficiently large d. As noted above, these results combined with the fact that relations (118) and (119) are indeed rigorous upper and lower bounds on S and η_c, respectively, for $d = 1$ provide strong theoretical arguments that these are rigorous bounds for all dimensions. Numerical simulations in sufficiently low dimensions discussed in Sec. VII also support these claims.

For large d, the pole $\eta_0^{(1)}$ has the following asymptotic behavior:

$$\eta_0^{(2)} = \frac{1}{2^d} - \frac{C_3}{2^{3d}} - \frac{C_4}{2^{4d}} + \frac{2C_3^2}{2^{5d}} + \mathcal{O}\left(\frac{C_3C_4}{2^{6d}}\right), \quad d \gg 1 \tag{120}$$

As expected, the first two terms in this expression match the exact asymptotic expansion (87). Since $|C_3|/2^{2d}$ and $|C_4|/2^{3d}$ tend to zero exponentially fast as $d \to \infty$ for both

TABLE III. Estimates of the percolation threshold η_c for overlapping hyperspheres as obtained from the lower bounds (98), (113), and (119), Percus-Yevick-like approximation (83) and simulation data[29] for dimensions two through eleven. The relevant trimer and tetramer statistics are obtained from Tables I and II.

d	η_c^{PY} from Eq. (83)	η_c	η_c^L from Eq. (119)	η_c^L from Eq. (113)	η_c^L from Eq. (98)
2		1.1282	0.748742...	0.604599...	0.250000...
3	0.500000...	0.3418	0.271206...	0.235294...	0.125000...
4	0.138093...	0.1300	0.111527...	0.100766...	0.0625000...
5	0.0546701...	0.0543	0.0488542...	0.0453257...	0.0312500...
6	0.0236116...	0.02346	0.0222117...	0.0209930...	0.0156250...
7	0.0106853...	0.0105	0.0103452...	0.00991018...	0.00781250...
8	0.00497795...	0.00481	0.00489917...	0.00474036...	0.00390625...
9	0.00236383...	0.00227	0.00234800...	0.00228912...	0.00195312...
10	0.00113725...	0.00106	0.00113534...	0.00111326...	0.000976562...
11	0.000552172...	0.000505	0.000552682...	0.000544338...	0.000488281...

hyperspheres and hypercubes [cf. Eqs. (53), (57), (61), and (64)], the lower bound (119) tends to the exact asymptotic result of $1/2^d$ in this limit [cf. Eq. (69)] for these models.

E. [*n*, 1] Padé approximant

We expect that higher order [n, 1] Padé approximants ($n \geq 3$) of S also provide lower bounds on η_c for $d \geq 2$ for $n \geq 3$ and relatively low d provided that successive density coefficients S_{n+1} and S_{n+2} remain positive. For example, we have verified that $S_{[3,1]}$ yields lower bounds on η_c for $d = 2$ and $d = 3$. However, as noted earlier, because we expect S_n to become negative at some large value of n for $d = 2$ and $d = 3$, $S_{[n,1]}$ cannot always yield lower bounds on η_c for relatively low dimensions such that $d \geq 2$. In the limit $d \to \infty$, we have shown that the S_n are all positive [cf. Eq. (75)], and hence, it is possible that in sufficiently high d, $S_{[n,1]}$ gives lower bounds on η_c for any n. See also related discussion in Sec. IX.

VII. RESULTS FOR OVERLAPPING HYPERSPHERES

In Table III, we compare the lower bounds (98), (113), and (119) on the percolation threshold η_c, and Percus-Yevick-like approximation (83) for η_c for overlapping hyperspheres to the corresponding simulation data obtained by Krüger[29] for dimensions two through eleven. Although more precise values of η_c have been determined in two[43,44] and three[45,46] dimensions, Krüger claims to have obtained estimates for η_c that are accurate essentially up to the number of significant figures indicated in Table III for all of the considered dimensions. By comparing the bounds to the simulation data, one can see that the bounds become progressively tighter as the space dimension increases (for reasons already mentioned in Sec. VI) and that the lower bound derived from the [2, 1] provides an excellent estimate for higher dimensions. Observe also that the Percus-Yevick-like estimate (83) of η_c bounds the simulation data from above for dimensions two through nine. Since it becomes increasingly challenging to estimate percolation thresholds from simulations in high dimensions, it is not surprising that the simulation data fall slightly below the putative lower bound (119) for $8 \leq d \leq 11$, which becomes asymptotically exact in high dimensions. Nonetheless, the quality of the simulation data is quite high.

This is to be contrasted with the simulation data reported by Wagner *et al.*[30] for hyperspheres up to dimension 20. In particular, they find that $2^d\eta_c$ incorrectly is a non-monotonic function of dimension; they find that $2^d\eta_c$ decreases as a function of d up to dimension nine, increases at $d = 10$ above its value at $d = 9$, and then decreases again for larger values of d. By contrast, the simulation data of Krüger[29] for $2^d\eta_c$ is a monotonic function of d, which is consistent with our theoretical results.

Figure 5 depicts the data listed in Table III graphically. It is seen that as the order of the Padé approximant increases, the corresponding estimates of the threshold become progressively better for any fixed dimension. All of the theoretical estimates, including the Percus-Yevick-like approximation (Eq. (83)), improve in accuracy as the space dimension increases.

Figures 6–8 plot theoretical estimates of the inverse of the mean cluster number S^{-1} as a function of the reduced

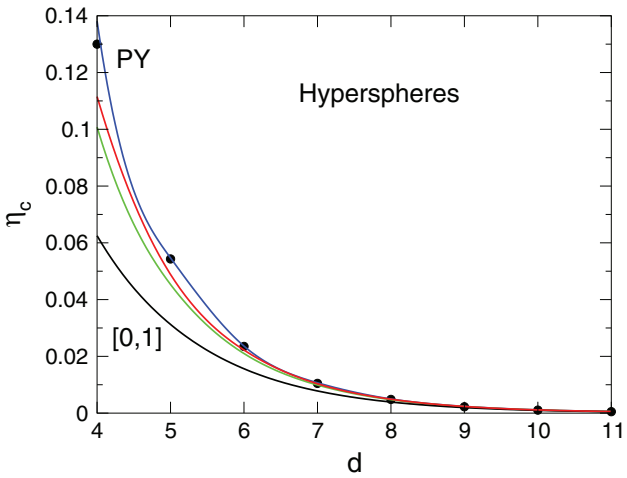

FIG. 5. Percolation threshold η_c versus dimension d for overlapping hyperspheres as obtained from the lower bounds (98) (lowermost curve), (113) and (119), Percus-Yevick-like approximation (83) (uppermost curve)), and simulation data (black circles).[29]

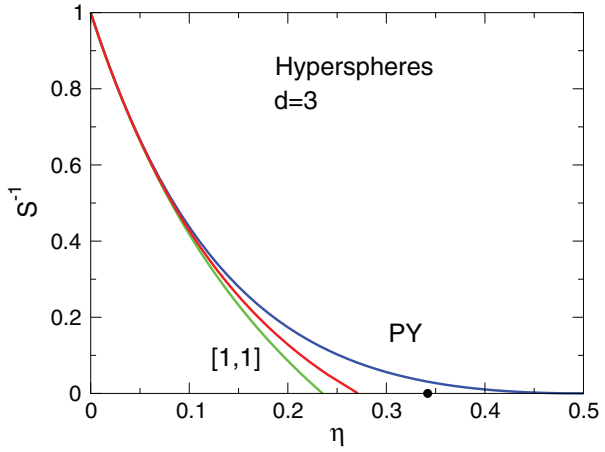

FIG. 6. Lower bounds on the inverse of the mean cluster number S^{-1} versus reduced density η for overlapping hyperspheres for $d = 3$ as obtained from inequalities (112) (lowermost curve) and (118). Included is the corresponding estimate obtained from the Percus-Yevick-like approximation (79) (upppermost curve). The filled black circle shows the threshold η_c determined numerically in Ref. 29.

density η for dimensions 3, 6, and 11, respectively. These include those expressions for S^{-1} obtained from the [1, 1] and [2, 1] Padé approximants of S [cf. (Eqs. (112) and (118))], which bound S^{-1} from below, and the Percus-Yevick-like approximation (Eq. (79)). These figures clearly illustrate that the theoretical estimates for the inverse mean cluster number become increasingly more accurate as the space dimension increases. Indeed, for $d = 11$, all of the theoretical estimates essentially coincide with one another for all densities up to the threshold. This is not surprising, since all of these estimates become asymptotically exact as the space dimension becomes large.

We use the threshold estimate obtained from the [2, 1] Padé approximant of S as the basis for an accurate analytical approximation for η_c that applies across all dimensions for hyperspheres. Specifically, we fit the following function to the simulation data for $2 \le d \le 7$:

$$\eta_c \approx \left(1 + \frac{b_1}{d^2} + \frac{b_2}{d^4}\right) \eta_0^{(2)}. \tag{121}$$

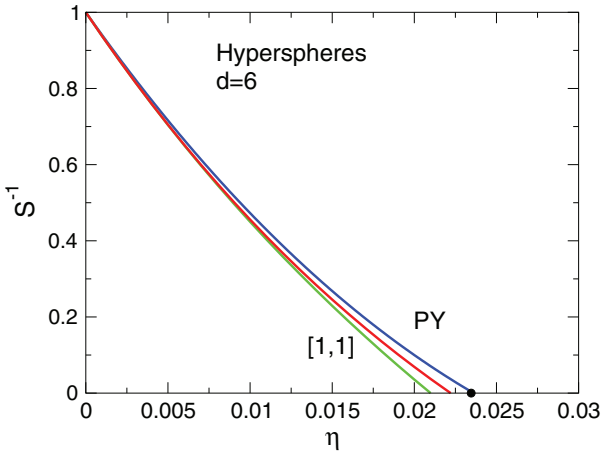

FIG. 7. As in Fig. 6, except for $d = 6$.

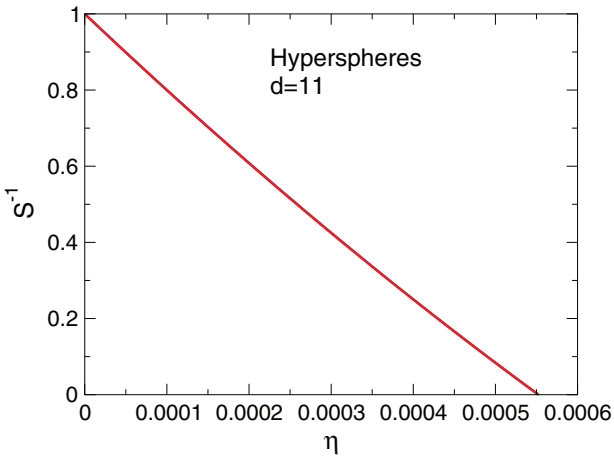

FIG. 8. As in Fig. 6, except for $d = 11$. Note that all of the theoretical estimates essentially coincide for this dimension on the scale of this figure.

We find that $b_1 = 2.05801$ and $b_2 = 3.15983$, and correlation coefficient equal to 0.997906. Here, $\eta_0^{(2)}$ is the pole for [2, 1] Padé approximant explicitly given by Eq. (119).

VIII. RESULTS FOR OVERLAPPING HYPERCUBES

In Table IV, we present the lower bounds (98), (113), and (119) on the percolation threshold η_c, and Percus-Yevick-like approximation (83) for η_c for overlapping oriented hypercubes for dimensions two through twelve, and compare to the corresponding simulation data for dimensions two and three[47] as well as four.[30] By comparing the bounds to the simulation data one can see that the bounds become progressively tighter as the space dimension increases, as in the case of hyperspheres, and that the lower bound derived from the [2, 1] approximant provides an excellent estimate for higher dimensions. Unlike in the case of hyperspheres, the Percus-Yevick-like estimate (83) of η_c always bounds the simulation data from below. Like the case of hyperspheres, this approximation becomes essentially indistinguishable from the estimate obtained from the [2, 1] approximant in the higher dimensions. We see that the threshold for hyperspheres is always above that for hypercubes as obtained from our theoretical estimates. Given that the qualitative trends for the thresholds and mean cluster number are similar for hypercubes and hyperspheres, we do not provide plots that are analogous to Figs. 5–8.

Note that Wagner *et al.*[30] also reported numerical estimates of η_c for $5 \le d \le 15$. However, we do not list those values in Table IV, since they violate the lower bound (119). Another reason why this simulation data is questionable in high dimensions is that $2^d \eta_c$ is incorrectly found to be a nonmonotonic function of d (as they found for hyperspheres); the authors find that it first decreases as d increases for $2 \le d \le 9$ and then increases as d increases for $10 \le d \le 15$. Indeed, they incorrectly conclude from their data that hyperspheres have lower thresholds than hypercubes in higher dimensions while the reverse is true at lower dimensions. The fact is that hypercubes always have a lower threshold than hyperspheres for any fixed finite dimension,

TABLE IV. Estimates of the percolation threshold η_c for overlapping hypercubes as obtained from the lower bounds (98), (113), and (119) and Percus-Yevick-like approximation (83) for dimensions two through eleven. Included for comparison are corresponding simulation data for dimensions two through four.[30,47] The relevant trimer and tetramer statistics are obtained from Tables I and II.

d	η_c^{PY} from Eq. (83)	η_c	η_c^L from Eq. (119)	η_c^L from Eq. (113)	η_c^L from Eq. (98)
2		1.098	0.732558...	0.571428...	0.250000...
3	0.267949...	0.3248	0.256680...	0.216216...	0.125000...
4	0.101137...	0.12	0.103286...	0.0914285...	0.0625000...
5	0.0431986...		0.0447161...	0.0409731...	0.0312500...
6	0.0195737...		0.0202386...	0.0190080...	0.0156250...
7	0.00916745...		0.0094301...	0.00901598...	0.00781250...
8	0.00438238...		0.00448213...	0.00434082...	0.00390625...
9	0.00212321...		0.00216025...	0.00211167...	0.00195312...
10	0.00103805...		0.00105159...	0.00103483...	0.000976562...
11	0.000510713...		0.000515602...	0.000509813...	0.000488281...

and the thresholds of these two systems approach one another in the limit $d \to \infty$, as noted above.

As in the case of hyperspheres, we use the percolation threshold estimate obtained from the [2, 1] Padé approximant of S to obtain an accurate analytical approximation for η_c that applies across all dimensions for hypercubes. In particular, we fit the following function to the simulation data for $2 \le d \le 4$:

$$\eta_c \approx \left(1 + \frac{b_1}{d^2} + \frac{b_2}{d^4}\right) \eta_0^{(2)}. \tag{122}$$

We find that $b_1 = 2.73808$ and $b_2 = -2.97382$, and correlation coefficient equal to 0.999938. Here $\eta_0^{(2)}$ is the pole for [2, 1] Padé approximant explicitly given by Eq. (119).

IX. DISCUSSION

We have shown that lower order Padé approximants of the mean cluster number S of the form $[n, 1]$ (where $n = 0$, 1, and 2) provide upper bounds on S and, hence, yield corresponding lower bounds on the threshold η_c for overlapping hyperspheres and oriented hypercubes in any dimension d. These estimates and the Percus-Yevick-like approximations already become accurate in relatively low dimensions, improve in accuracy as d increases, and become exact asymptotically, i.e., η_c tends to zero as 2^{-d} as $d \to \infty$. The latter result applies for any overlapping system of identical oriented d-dimensional convex particles that possess central symmetry[48] (e.g., spheres, cubes, regular octahedra, and regular icosahedra).

Note that the aforementioned trends and asymptotic results will hold for overlapping particles of *arbitrary shape and orientational distribution* when appropriately generalized. For example, for identical overlapping particles of general anisotropic shape of volume v_1 with specified probability distribution of orientations in d dimensions, the simplest lower bound on η_c inequality (98) and on $\mathcal{N}_c$ inequality (99) generalizes as follows:

$$\eta_c \ge \frac{v_1}{v_{\rm ex}}, \tag{123}$$

$$\mathcal{N}_c \equiv \eta_c \frac{v_{\rm ex}}{v_1} \ge 1, \tag{124}$$

where

$$v_{\rm ex} = \int_{\mathbb{R}^d} f(\mathbf{r}, \boldsymbol{\omega}) p(\boldsymbol{\omega}) d\mathbf{r} d\boldsymbol{\omega}, \tag{125}$$

$f(\mathbf{r}, \boldsymbol{\omega})$ is still the exclusion-region indicator function, $\mathbf{r}$ and $\boldsymbol{\omega}$ is the centroidal position and orientation of one particle, respectively, with respect to a coordinate system at the centroid of the other particle with some fixed orientation, and $p(\boldsymbol{\omega})$ is the orientational probability density function. Moreover, in the high-dimensional limit for any convex particle shape, we obtain the exact asymptotic results,

$$\eta_c \sim \frac{v_1}{v_{\rm ex}}, \quad d \to \infty, \tag{126}$$

$$\mathcal{N}_c \sim 1, \quad d \to \infty. \tag{127}$$

Exclusion volumes are known for a variety of convex nonspherical shapes that are randomly oriented in two and three dimensions,[49,50] which must be necessarily larger than the corresponding values when all of the particles are aligned and possess central symmetry, in which case $v_{\rm ex}/v_1 = 2^d$, independent of the particle shape. For example, for randomly oriented rectangles,[50] $v_{\rm ex}/v_1 = 2 + (\beta + 1)^2/(\pi\beta)$, and ellipses,[50] $v_{\rm ex}/v_1 = 2 + 4\beta E(1 - \beta^{-2})^2/\pi^2$, where β is the aspect ratio and $E(x) = \int_0^{\pi/2} dt(1 - x \sin^2(t))^{1/2}$ is the complete elliptic integral of the second kind. For randomly oriented cubes,[49] $v_{\rm ex}/v_1 = 11$, and spheroids,[49] $v_{\rm ex}/v_1$ is an analytical relation given in terms of the aspect ratio, which in the prolate "needle-limit" yields $v_{\rm ex}/v_1 \sim 3\pi\beta/4$ ($\beta \gg 1$). Thus, lower bound (123) for randomly oriented cubes and needles yields $\eta_c \ge 1/11 = 0.09090909...$ and $\eta_c \ge 4/(3\pi\beta) = (0.424413181...)/\beta$, respectively. These values should be compared to the corresponding simulation values of $\eta_c = 0.2168$ (Ref. 47) and $\eta_c = 0.6/\beta$,[51] respectively (see Refs. 51 and 52 for numerical estimates of η_c for other spheroid aspect ratios). Note that in the case of three-dimensional needles, the lower bound (123) is considerably sharper than for three-dimensional spheres. Indeed, the lower bound (123) improves in accuracy in any fixed dimension as the particle shape becomes more anisotropic. Balberg *et al.*[53] have suggested that $\mathcal{N}_c$ is an approximant invariant for overlapping particles of general shape in two and three dimensions. Simulations have shown this not to be an invariant[47,51,54] in

these low dimensions. However, the asymptotic result (127) reveals that $\mathcal{N}_c$ is an invariant, with value unity, in the high-dimensional limit regardless of the shape of the convex particle. The lower bound on η_c for randomly oriented convex nonspherical particles (including Archimedean polyhedra[48,55]) corresponding to inequality (98) will be the subject of a future study.

We have already noted the remarkable duality between continuum percolation of overlapping particles and corresponding hard particles in equilibrium in high dimensions (and low densities regardless of the dimension). There is yet another amazing manifestation of this duality involving the percolation threshold for continuum percolation and the limiting density for a class of disordered hard-particle systems. For simplicity of discussion, we will focus on overlapping hyperspheres and the corresponding packing of disordered hard hyperspheres in high dimensions. We have seen that the percolation threshold η_c of the former system tends to 2^{-d} as $d \to \infty$. The dual statement is that there is a variety of disordered hard hyperspheres whose upper limiting packing fraction ϕ (fraction of space covered by the hard hyperspheres) is also 2^{-d} in this high-dimensional limit, some of which we will now describe.

First, it has been shown that the pressure of an equilibrium hard-hypersphere packing is exactly given by the first two terms of its asymptotic low-density expansion for some positive density interval $[0, \phi_0]$ as $d \to \infty$.[41,56] Frisch and Percus[41] have argued that $\phi_0 = 2^{-d}$, which implies that the pair correlation function $g_2(r)$ tends to a unit-step function, i.e., $g_2(r) \to \Theta(r - D)$, where D is the hypersphere diameter. [Recall that the dual statement for the percolation problem is that the pair connectedness function tends to the complimentary unit-step function, i.e., $P(r) \to \Theta(D - r)$ (see Eq. (106)).] According to the *decorrelation principle*, which states that unconstrained correlations that exist in low dimensions must vanish in the high-dimensional limit,[35] this implies that 2^{-d} is the high-dimensional asymptotic limit for the packing fraction of the *freezing point* of a hard hypersphere system. Why? Because only short-range correlations characteristic of disordered states along the stable fluid branch (rather than the long-ranged correlations describing states along the stable crystal branch) can decorrelate to a unit-step function $\Theta(r - D)$. This outcome concerning the asymptotic form of the freezing-point density does not appear to have noted or appreciated before. A second example is provided by the so-called "ghost" random sequential addition packing, which is an exactly solvable disordered hard hypersphere model for any dimension d whose maximal packing fraction is again given by 2^{-d}.[57] This *nonequilibrium* packing again possesses a pair correlation function that has the asymptotic behavior $g_2(r) \to \Theta(r - D)$. Third, it has been shown that certain so-called g_2-invariant processes in which $g_2(r) = \Theta(r - D)$ are achieved in the high-dimensional limit with maximal packing fraction $\phi \to 2^{-d}$.[35,58] It is important to note that there exists hard-hypersphere packings with packing fractions that exceed 2^{-d} in high dimensions, but with pair correlation functions that are not simple unit step functions.[35,59]

Our analysis enables us to draw some new conclusions about the radius of convergence of the density expansion (20) of the mean cluster number S as a function dimension. First, note that this radius of convergence in the high-dimensional limit corresponds to the percolation threshold because the coefficients of the density expansion of the exact asymptotic expression (75) for the mean cluster number are all positive. As we already observed in Sec. II B, this is generally not the case for $d \geq 2$ and sufficiently low d, where we expect the closest singularities to lie on the negative real axis. However, in one dimension, we see from Sec. VI A that radius of convergence indeed corresponds to η_c. Thus, the closest singularities for the density expansion of S shifts from the positive real axis to the negative real axis in going from one to two dimensions, remain on the negative real axis for sufficiently low dimensions $d > 2$, and eventually move back to the positive real axis for sufficiently large d.

As discussed in Sec. VIII, our theoretical analysis revealed fundamental deficiencies in the dependence of the percolation threshold η_c as a function of d for overlapping oriented hypercubes reported in the numerical work of Ref. 30. In future work, we will report simulation results for overlapping oriented hypercubes for d up to 15 in which $2^d\eta_c$ is a decreasing monotonic function of dimension d that satisfies the lower bound (119) and has a threshold η_c that always lies below the corresponding value for overlapping hyperspheres. Moreover, in a follow-up investigation, we will show that the lower order Padé approximants studied here lead also to bounds on the percolation threshold for lattice-percolation models in arbitrary dimension.

ACKNOWLEDGMENTS

The author is grateful to Yang Jiao and Cedric Gommes for their critical reading of this manuscript. This work was supported by the Materials Research Science and Engineering Center Program of the National Science Foundation under Grant No. DMR-0820341.

APPENDIX: HIGH-DIMENSIONAL GENERALIZATION OF THE PERCUS-YEVICK APPROXIMATION FOR HARD HYPERSPHERES AND HYPERCUBES

The Percus-Yevick approximation for the pressure of a three-dimensional hard-sphere fluid via the "compressibility" route is given by

$$\frac{p}{\rho k_B T} = \frac{1 + \eta + \eta^2}{(1 - \eta)^3}, \tag{A1}$$

where η is still the reduced density defined by Eq. (1) but here also represents the fraction of space covered by the hard spheres (denoted by ϕ in Sec. IX), since, unlike the continuum percolation model, overlap of particles is prohibited. This approximation for the equation of state, which is exact up through the third virial coefficient, is slightly more accurate than the resulting Percus-Yevick approximation via the "pressure" equation. A means of generalizing this result to other space dimensions was proposed by Torquato in his consideration of nearest-neighbor statistics for the equilibrium hard-disk fluid.[60] Specifically, this procedure presumed the form $p/(\rho k_B T) = (1 + a_1\eta + a_2\eta^2)/(1 - \eta)^2$ and determined the

coefficients a_1 and a_2 so that the equation of state was exact up through the third virial coefficient, implying $a_1 = 0$ and $a_2 = 0.1280\ldots$. For general d, this Percus-Yevick-like approximation yields

$$\frac{p}{\rho k_B T} = \frac{1 + a_1\eta + a_2\eta^2}{(1-\eta)^d}. \tag{A2}$$

where, using Eqs. (28) and (29),

$$a_1 = \frac{B_2}{v_1(D/2)} - d = \frac{C_2}{2} - d, \tag{A3}$$

$$a_2 = \frac{d(d-1)}{2} - d2^{d-1} + \frac{B_3}{v_1(D/2)^2} = \frac{d(d-1)}{2} - \frac{C_2 d}{2} - \frac{C_3}{3}. \tag{A4}$$

We see that for three-dimensional spheres, we recover Eq. (A1) with $a_1 = a_2 = 1$, and for one-dimensional hard rods, we recover the exact result with $a_1 = a_2 = 0$. The appropriate dimensionless pressure for d-dimensional hard hypercubes is obtained from Eq. (A1) but with the corresponding third virial coefficient B_3 for this system.

[1] C. J. Brinker and G. W. Scherer, *Sol-Gel Science: The Physics and Chemistry of Sol-Gel Processing* (Academic, New York, 1990).
[2] D. Stauffer and A. Aharony, *Introduction to Percolation Theory* (Taylor & Francis, London, 1992).
[3] M. Sahimi, *Applications of Percolation Theory* (Taylor & Francis, London, 1994).
[4] S. Torquato, *Random Heterogeneous Materials: Microstructure and Macroscopic Properties* (Springer-Verlag, New York, 2002).
[5] S. W. Haan and R. Zwanzig, J. Phys. A **10**, 1547 (1977).
[6] A. Coniglio, U. De Angelis, and A. Forlani, J. Phys. A **10**, 1123 (1977).
[7] Y. C. Chiew and E. D. Glandt, J. Phys. A **16**, 2599 (1983).
[8] G. Stell, J. Phys. A **17**, L855 (1984).
[9] T. DeSimone, R. M. Stratt, and S. Demoulini, Phys. Rev. Lett. **56**, 1140 (1986).
[10] A. K. Sen and S. Torquato, J. Chem. Phys. **89**, 3799 (1988).
[11] S. Torquato, J. D. Beasley, and Y. C. Chiew, J. Chem. Phys. **88**, 6540 (1988).
[12] L. A. Fanti, E. D. Glandt, and Y. C. Chiew, J. Chem. Phys. **89**, 1055 (1988).
[13] S. B. Lee and S. Torquato, J. Chem. Phys. **89**, 6427 (1988).
[14] G. Grimmet, *Percolation* (Springer-Verlag, New York, 1989).
[15] J. A. Given and G. Stell, J. Stat. Phys. **39**, 981 (1990).
[16] J. A. Given, I. C. Kim, S. Torquato, and G. Stell, J. Chem. Phys. **93**, 5128 (1990).
[17] M. D. Penrose, Adv. Appl. Prob. **23**, 536 (1991).
[18] E. Cinlar and S. Torquato, J. Stat. Phys. **78**, 827 (1995).
[19] J. Quintanilla and S. Torquato, Phys. Rev. E **54**, 5331 (1996); *ibid.* **56**, 3732 (1997) (Erratum).
[20] S. Prager, Phys. Fluids **4**, 1477 (1961).
[21] R. A. Reck and S. Prager, J. Chem. Phys. **42**, 3027 (1965).
[22] H. L. Weissberg and S. Prager, Phys. Fluids **13**, 2958 (1970).
[23] J. G. Berryman, J. Phys. D. **18**, 585 (1985).
[24] S. Torquato, J. Chem. Phys. **84**, 6345 (1986).
[25] S. Torquato, F. Lado, and P. A. Smith, J. Chem. Phys. **86**, 6388 (1987).
[26] J. Rubinstein and S. Torquato, J. Chem. Phys. **88**, 6372 (1988).
[27] J. Rubinstein and S. Torquato, J. Fluid Mech. **206**, 25 (1989).
[28] Note that if the reduced density η is fixed for both the overlapping hypersphere and hypercube systems, as defined in the text, the number density for the former ρ_S is related to that for the latter ρ_C according to the expression $\rho_S/\rho_C = (2/\pi)^d\Gamma(1 + d/2)$. Thus, the ratio ρ_S/ρ_C grows superexponentially fast as d becomes large under these conditions.
[29] A. Krüger, Ph.D. dissertation, University of Bielefeld, Germany, 2003.
[30] N. Wagner, I. Balberg, and D. Klein, Phys. Rev. E **74**, 011127 (2006).
[31] S. B. Lee and S. Torquato, Phys. Rev. A **41**, 5338 (1990).
[32] M. F. Sykes, J. L. Martin, and J. W. Essam, J. Phys. A **6**, L306 (1973).
[33] Our use of the term "duality" is different from its usual usage in percolation theory in which it refers to relationships between certain two-dimensional lattices; see, for example, Refs. 3, 4, and 14.
[34] J. P. Hansen and I. R. McDonald, *Theory of Simple Liquids* (Academic, New York, 1986).
[35] S. Torquato and F. H. Stillinger, Exp. Math. **15**, 307 (2006).
[36] S. Torquato and F. H. Stillinger, Phys. Rev. E **68**, 041113 (2003).
[37] B. R. A. Nijboer and L. Van Hove, Phys. Rev. **85**, 777 (1952).
[38] J. S. Rowlinson, Mol. Phys. **7**, 593 (1964).
[39] N. Clisby and B. McCoy, J. Stat. Phys. **114**, 1343 (2004).
[40] I. Lyberg, J. Stat. Phys. **119**, 747 (2005).
[41] H. L. Frisch and J. K. Percus, Phys. Rev. E **60**, 2942 (1999).
[42] The fact that (103) implies a lower bound on η_c was not observed in Ref. 15.
[43] J. Quintanilla, S. Torquato, and R. M. Ziff, J. Phys. A **33**, L399 (2000).
[44] J. A. Quintanilla and R. M. Ziff, Phys. Rev. E **76**, 051115 (2007).
[45] M. D. Rintoul and S. Torquato, J. Phys. A **30**, L585 (1997).
[46] C. D. Lorenz and R. M. Ziff, J. Chem. Phys. **114**, 3659 (2000).
[47] D. R. Baker, G. Paul, S. Sreenivasan, and H. E. Stanley, Phys. Rev. E **66**, 046136 (2002).
[48] S. Torquato and Y. Jiao, Phys. Rev. E **80**, 041104 (2009).
[49] A. Isihara, J. Chem. Phys. **18**, 1446 (1950); T. Kihara, Rev. Mod. Phys. **25**, 831 (1953).
[50] T. Boublík, Mol. Phys. **29**, 421 (1975); G. Tarjus, P. Viot, S. Ricci, and J. Talbot, *ibid.* **73**, 773 (1991).
[51] E. J. Garboczi, K. A. Snyder, J. F. Douglas, and M. F. Thorpe, Phys. Rev. E **52**, 819 (1995).
[52] Y.-B. Yi and A. M. Sastry, Proc. R. Soc. London, Ser. A **460**, 2353 (2004).
[53] I. Balberg, C. H. Anderson, S. Alexander, and N. Wagner, Phys. Rev. B **30**, 3933 (1984).
[54] W. Xia and M. F. Thorpe, Phys. Rev. A. **38**, 2650 (1988).
[55] Y. Jiao and S. Torquato, J. Chem. Phys. **135**, 151101 (2011).
[56] D. Wyler, N. Rivier, and H. L. Frisch, Phys. Rev. A **36**, 2422 (1987).
[57] S. Torquato and F. H. Stillinger, Phys. Rev. E **73**, 031106 (2006).
[58] S. Torquato and F. H. Stillinger, J. Phys. Chem. B **106**, 8354 (2002); *ibid.* **106**, 11406 (2002) (Erratum).
[59] H. Cohn and N. Elkies, Ann. Math. **157**, 689 (2003).
[60] S. Torquato, Phys. Rev. Lett. **74**, 2156 (1995); Phys. Rev. E **51**, 3170 (1995). In these papers, the dimensionless pressure (Eq. (A2)) was denoted by a_0, and for $d = 2$ contained a typographical error, namely, a_0 should be equal to $(1 - 0.128\,\phi^2)/(1 - \phi)^2$ (where ϕ is the packing fraction).